

## Systematic study of the nuclear potential through high precision back-angle quasi-elastic scattering measurements

L. R. Gasques,<sup>1</sup> M. Evers,<sup>1</sup> D. J. Hinde,<sup>1</sup> M. Dasgupta,<sup>1</sup> P. R. S. Gomes,<sup>2</sup> R. M. Anjos,<sup>2</sup> M. L. Brown,<sup>1</sup>  
M. D. Rodríguez,<sup>1</sup> R. G. Thomas,<sup>1</sup> and K. Hagino<sup>3</sup>

<sup>1</sup>*Department of Nuclear Physics, Research School of Physical Sciences and Engineering, Australian National University, Canberra, ACT 0200, Australia*

<sup>2</sup>*Instituto de Física, Universidade Federal Fluminense, Av. Litorânea s/n, 24210-340 Niteroi, Rio de Janeiro, Brazil*

<sup>3</sup>*Department of Physics, Tohoku University, Sendai 980-8578, Japan*

(Received 18 May 2007; published 27 August 2007)

High precision quasi-elastic scattering excitation functions have been measured at energies well below the Coulomb barrier for the reactions of  $^{32}\text{S}$  with  $^{208}\text{Pb}$ ,  $^{197}\text{Au}$ ,  $^{186}\text{W}$ , and  $^{170}\text{Er}$ . Single-channel and coupled-channels calculations have been performed to extract the diffuseness parameter of the nuclear potential. For the reactions involving near-spherical targets, both theoretical analyses give the same diffuseness parameter. On the other hand, for deformed systems, couplings are important even at deep sub-barrier energies. In general, the effect of couplings is to reduce the diffuseness parameter value extracted from a single-channel potential. Single-channel fits to quasi-elastic scattering data result in  $a = 0.72\text{--}0.82$  fm, whereas coupled-channels calculations give diffuseness parameters in the range  $0.58\text{--}0.75$  fm.

DOI: [10.1103/PhysRevC.76.024612](https://doi.org/10.1103/PhysRevC.76.024612)

PACS number(s): 25.70.Bc, 21.30.Fe, 24.10.Ht, 24.10.Eq

### I. INTRODUCTION

Knowledge of the nuclear potential is critical to describing many aspects of nuclear collisions. For heavy-ion reactions, the Woods-Saxon (WS) form, which is characterized by the depth  $V_0$ , radius  $r_0$ , and diffuseness  $a$  parameters, has been widely adopted to describe the nuclear potential. Elastic and inelastic scatterings, which are sensitive to the nuclear potential in the surface region [1,2], are able to probe the surface diffuseness of the nuclear potential. In general, a diffuseness of around 0.63 fm seems to be adequate to describe elastic and inelastic scattering data [1–6]. Contrary to this result, large diffuseness parameters, ranging between 0.75 and 1.5 fm, are required to fit a large number of precision fusion excitation functions recently measured at energies around the Coulomb barrier [7]. Elastic scattering and fusion differ in that they explore different regions of the nuclear potential, the former probing much larger separation distances than the latter. Possible explanations for the differences in diffuseness include the possibility that the nuclear potential deviates from the WS shape at closer distances or that dissipative processes play a role [7,8]. However, a definitive reason for the large discrepancies in diffuseness parameter extracted from elastic scattering and fusion analyses has still to be determined.

It has recently been shown that precise measurements of deep sub-barrier quasi-elastic excitation functions at backward angles provide a means of studying the diffuseness parameter of the WS nuclear potential [9–11], apparently without sensitivity to whether couplings are included in the calculations. This aspect makes the approach very attractive. The sensitivity of the back-angle quasi-elastic scattering to the tail of the nuclear potential can be easily visualized in a classical picture where the nuclear force deflects Rutherford trajectories to more forward angles, resulting in a slight depletion of quasi-elastic scattering flux at backward angles. Generally, the

quasi-elastic cross section is defined as the sum of the elastic scattering and all other peripheral reaction processes, and at sub-barrier energies it can be associated with the total outgoing (reflected) flux of particles. It is known that couplings of the relative motion of projectile and target nuclei to internal nuclear degrees of freedom are significant for heavy-ion reactions at near-barrier energies [12,13]. This results in a distribution of fusion barrier energies and increases the fusion cross section. At deep sub-barrier energies, where the loss of quasi-elastic flux to fusion is negligible, the channel couplings affect the distribution of flux only among the quasi-elastic channels. Therefore, at such low energies, one might expect a good description of quasi-elastic scattering by a single-channel potential model.

In a recent publication [10], Washiyama *et al.* performed a systematic study of the surface diffuseness parameter using sub-barrier quasi-elastic excitation functions measured at backward angles for a number of reactions. The best fit to the experimental data was obtained with a diffuseness parameter of around 0.60 fm for systems involving heavy near-spherical nuclei, while large values for  $a$ , in the range  $a = 0.8\text{--}1.1$  fm, were required to fit reactions with heavy deformed target nuclei. However, the quasi-elastic scattering data fitted in that work were not taken from measurements carried out for that purpose. Ideally, data are required with much higher precision, extending to deeper sub-barrier energies than had previously been the case for measurements of quasi-elastic scattering.

In this work, we present measurements of precise excitation functions for quasi-elastic scattering of  $^{32}\text{S}$  incident on  $^{208}\text{Pb}$ ,  $^{197}\text{Au}$ ,  $^{186}\text{W}$ , and  $^{170}\text{Er}$ . The cross sections were determined with statistical accuracy of 0.3–0.5%, at energies ranging from 0.54 to 0.95 of the respective fusion barriers  $V_B$ . Both near-spherical ( $^{208}\text{Pb}$ ,  $^{197}\text{Au}$ ) and deformed ( $^{186}\text{W}$ ,  $^{170}\text{Er}$ ) target nuclei were included to investigate the conclusions of

Ref. [10]. As reported in Ref. [7], the diffuseness parameter required to reproduce fusion data shows a strong increase with increase in the reaction charge product  $Z_1Z_2$ . The measurements were carried out using a  $^{32}\text{S}$  projectile nucleus to give a reasonably large value of  $Z_1Z_2$ , without the poor energy resolution of the silicon detector that could occur with substantially heavier projectiles. The main goal of this work is to perform a careful analysis of these high precision quasi-elastic scattering data, and explore experimental and analysis methods to determine the diffuseness parameter of the WS nuclear potential.

## II. EXPERIMENTAL METHOD

The experiments were performed using  $^{32}\text{S}$  beams from the 14UD tandem accelerator at the Australian National University. Thin targets (100–200  $\mu\text{g}/\text{cm}^2$  thick) of self-supporting  $^{197}\text{Au}$ , and of  $^{208}\text{PbS}$ ,  $^{186}\text{W}$ , and  $^{170}\text{Er}$  evaporated onto 15–20  $\mu\text{g}/\text{cm}^2$  C foils were used in the experiment. The measurements were carried out over the bombarding energy range of  $E_{\text{lab}} = 90\text{--}155$  MeV. The quasi-elastic reaction products were detected using an annular silicon surface barrier detector, placed 78 mm from the target, at a mean angle of  $174^\circ$  to the beam. Two Si surface barrier detectors (monitors), symmetrically placed about the beam axis at angles of  $\pm 30^\circ$ , were used to measure Rutherford scattering events for normalization purposes.

In making a useful systematic study of the experimental values of the diffuseness parameter, it is necessary to obtain deep sub-barrier quasi-elastic scattering data with high accuracy ( $\ll 1\%$ ). The following steps were taken to minimize possible systematic uncertainties in the measurements:

- (i) To avoid systematic errors from degradation of the detector response during the experiment, the beam energies were not increased monotonically, but randomly chosen. Additionally, for some energies, the measurements were repeated and found to be consistently reproducible.

- (ii) To maintain the same focal point of the incident particles at the target center, the  $^{32}\text{S}$  beam was tuned through a circular aperture with a diameter of 2 mm for each measured energy.
- (iii) The quasi-elastic scattering data were measured at energies ranging from  $E/V_B = 0.95$  down to  $E/V_B = 0.54$ ; to precisely determine the WS parameters, it is crucial that several data points are measured at sufficiently low energies to be insensitive to the nuclear potential.
- (iv) The backward-angle quasi-elastic measurements were performed with an annular counter, almost eliminating sensitivity to remaining shifts in beam-spot position or angle of the beam incident on the target.
- (v) Data were normalized using the two forward-angle monitor detectors, again minimizing sensitivity to beam spot position or beam angle.

At low energies, where the scattering is pure Rutherford, differences in the normalization factor between the targets are expected because of geometrical effects caused by axial distance variations between targets. Changes of  $\Delta z$  of 0.5 mm, with  $z$  being the direction of the incident beam, would result in variations in the normalization factor of  $\sim 1.3\%$ . Variations within this range between targets could be expected (and were observed) as a result of variations of target mounting and planarity.

Figure 1 shows typical energy spectra measured by the annular silicon detector placed at  $\theta = 174^\circ$  for the system  $^{32}\text{S}+^{208}\text{Pb}$ , at beam energies of 100 and 150 MeV. The peak corresponds to elastically scattered  $^{32}\text{S}$ . Increase of beam energy results in an increase of inelastic events and hence in more intensity in the low energy tail, as highlighted in Figs. 1(b) and 1(d), plotted with an expanded vertical scale. In the data analysis, the energy window for quasi-elastic was defined to include the elastic peak and the tail corresponding to all other peripheral processes. For all reactions, the quasi-elastic scattering counts were divided by the sum of the elastic scattering counts in the two forward-angle monitor detectors,

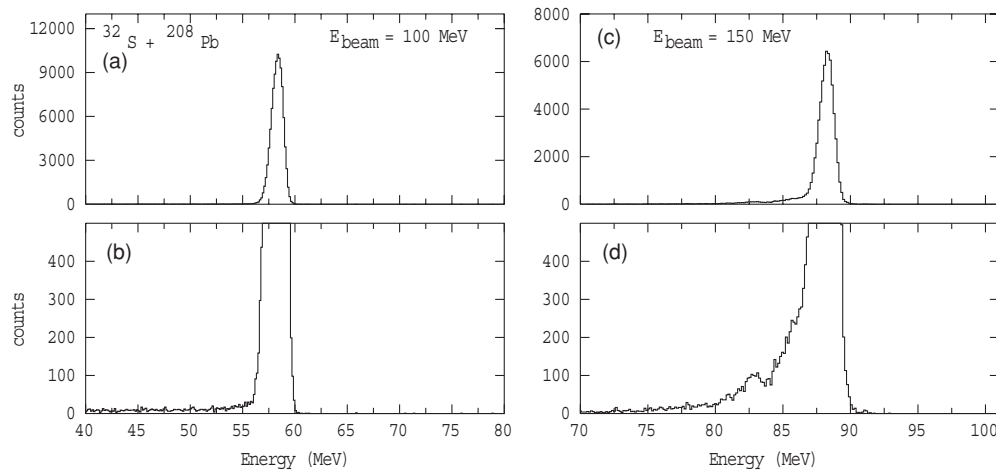


FIG. 1. Typical energy spectra from the annular silicon detector at  $\theta = 174^\circ$  for the system  $^{32}\text{S}+^{208}\text{Pb}$  measured at a beam energy of 100 MeV (a), (b) and 150 MeV (c), (d). Panels (b) and (d) show the same spectra as presented in (a) and (c) on an expanded vertical scale.

giving a quantity proportional to the ratio of the observed cross sections to Rutherford scattering ( $d\sigma_{q.e.}/d\sigma_{Ruth.}$ ).

### III. DATA ANALYSIS AND RESULTS

The investigation of the nuclear potential has been performed by comparing the measured large-angle quasi-elastic data with the expectations of single-channel and coupled-channels model calculations. Normalization of the experimental data is often achieved from one or a few low energy measurements, where the scattering is assumed to be Rutherford. This procedure can result in a systematic error in the absolute quasi-elastic scattering cross sections, leading to incorrect values for the diffuseness parameter. To avoid such systematic errors, in the present work the normalization factor between the theoretical calculation and the quasi-elastic data was allowed to vary freely in the  $\chi^2$ -fitting procedure. This aspect of the analysis procedure may explain differences in the diffuseness extracted in this work and those in Refs. [10,11]. To illustrate this point, we compare in Fig. 2 the  $^{32}\text{S}+^{197}\text{Au}$  quasi-elastic scattering excitation function obtained in this work (solid circles) with the data of Ref. [14] (open triangles) which were used to extract the diffuseness parameter in Ref. [10]. For the latter, the uncertainties in the data points have been omitted from the plot. Also shown in Fig. 2 by the filled triangles are the data of Ref. [14] multiplied by the normalization factor obtained from the  $\chi^2$ -fitting procedure. Allowing the normalization factor to vary results in good agreement between the present data and the data of Ref. [14]. The procedure adopted here is an improvement over those adopted in previous analyses [10,11], and the resulting

diffuseness parameters are therefore more reliable as they are insensitive to arbitrary normalization of experimental data. The better quality of the quasi-elastic scattering data obtained here is evident from Fig. 2. In this work, the relative uncertainties assigned to the experimental data points were determined only from statistics.

The single-channel and coupled-channels calculations were made using a WS form for the nuclear potential. In the calculations, an inner imaginary potential was used to account for the rather small internal absorption from barrier penetration. The values assumed for the parameters of the imaginary part of the potential ( $W = 30.0$  MeV;  $r_w = 1.0$  fm and  $a_w = 0.10$  fm) result in negligible strength in the surface region. As the imaginary part of the potential remained inside the Coulomb barrier, the quasi-elastic scattering cross section predictions were insensitive to variations of the imaginary potential parameters. The parameters of the WS real potential were searched to obtain the best fit to the quasi-elastic data, with the important constraint that the expected average fusion barrier energy for the different reactions had to be reproduced. Typically, the radius parameter  $r_0$  of the WS was kept between 1.0 and 1.1 fm, resulting in  $V_0$  ranging from 800 to 200 MeV, respectively. Within these limits, the determination of the diffuseness parameter is insensitive to the choice of  $r_0$ . For a given value of diffuseness, the potential depth parameter was varied so that the barrier energy was reproduced in each case. A small inconvenience appears because the experimental fusion barrier is only known for the  $^{32}\text{S}+^{208}\text{Pb}$  reaction [15]. However, using this information and the scaling parameter  $Z_1 Z_2 / (A_1^{1/3} + A_2^{1/3})$ , it was possible to determine the fusion barrier energy for the reactions of  $^{32}\text{S}$  with  $^{197}\text{Au}$  and  $^{186}\text{W}$ . Similarly, the  $^{34}\text{S}+^{168}\text{Er}$  experimental fusion data of Ref. [16] were used to determine the fusion barrier for the  $^{32}\text{S}+^{170}\text{Er}$  reaction. The fusion barrier energies for all the reactions studied in this work are given in Table I. The effects on the fits of changing the average barrier energy were investigated. For instance, for the  $^{32}\text{S}+^{197}\text{Au}$  reaction, the Akyüz-Winther nuclear potential [17] gives  $V_B = 141.2$  MeV, which is slightly larger than the average barrier energy presented in Table I. It turns out that changing the average barrier energy by  $\pm 1$  MeV essentially changes the best fitted diffuseness parameter by  $\pm 0.04$  fm. Note that the typical statistical uncertainties in the diffuseness parameter for all reactions are in the range of  $\pm 0.02$ – $0.04$  fm. The uncertainties in the diffuseness parameter were evaluated from the values at which the total chi-squared increases from the minimum by the minimum chi-squared per degree of freedom or by unity, whichever was larger.

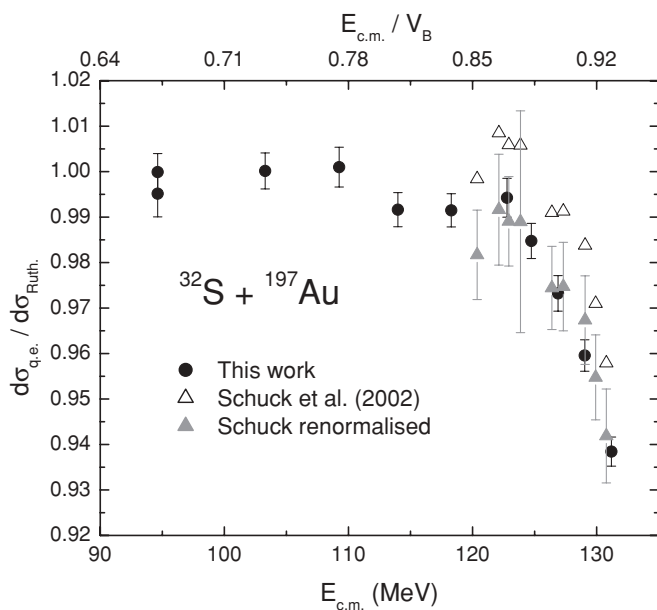


FIG. 2. Ratio of the quasi-elastic scattering to the Rutherford cross section for the  $^{32}\text{S}+^{197}\text{Au}$  reaction. The solid circles are the present data, whereas the open triangles refer to the data of Ref. [14]. The solid triangles are the renormalized data of Ref. [14]. See text for details.

TABLE I. Fusion barrier energy used to determine the nuclear potential for each value of diffuseness parameter.

Reaction	$V_B$ (MeV)	Method of determination
$^{32}\text{S}+^{208}\text{Pb}$	144.4	Determined from fusion data(Ref. [15])
$^{32}\text{S}+^{197}\text{Au}$	140.8	Scaled from the $^{32}\text{S}+^{208}\text{Pb}$ fusion data
$^{32}\text{S}+^{186}\text{W}$	133.5	Scaled from the $^{32}\text{S}+^{208}\text{Pb}$ fusion data
$^{32}\text{S}+^{170}\text{Er}$	123.7	Scaled from the $^{34}\text{S}+^{168}\text{Er}$ fusion data of Ref. [16]

To verify whether couplings can affect quasi-elastic scattering, coupled-channels calculations were performed with a modified version of the code CCFULL [18]. The introduction of couplings shifts the average barrier energy to a small extent. Thus, for calculations including couplings, the radius parameter of the real nuclear potential  $r_0$  was changed slightly so that the calculated fusion cross sections at energies well above barrier match the results obtained with a single-channel potential. This procedure is necessary to ensure that the average fusion barrier for the coupled-channels calculations remains the same as that for the single-channel case, and that the calculated fusion cross sections at energies well above barrier are not changed by the couplings. The deformation parameters  $\beta_\lambda$  associated with the multipolarity of the transitions  $\lambda$  were obtained from experimental electromagnetic transition probabilities  $B(E\lambda) \uparrow$  using

$$\beta_\lambda = \frac{4\pi}{3ZR^\lambda} \left[ \frac{B(E\lambda) \uparrow}{e^2} \right]^{1/2}, \quad (1)$$

where the radius of the target nucleus is taken to be  $R = r_t A^{1/3}$  fm. As reported in Ref. [19], the correct value of  $r_t$  to be adopted in the coupled-channels analysis is not entirely clear but is likely to lie somewhere between 1.06 and 1.20 fm. As the code CCFULL includes terms up to the second order with respect to  $\beta_2$  and to the first order in  $\beta_4$  [20] for the Coulomb interaction, the Coulomb couplings are independent of the choice of  $r_t$  [19]. For the reactions involving near-spherical targets studied in this paper, the effect of using  $r_t = 1.06$  or  $r_t = 1.20$  fm on the determination of the diffuseness parameter is negligible. The implications of varying  $r_t$  in the  $^{32}\text{S}+^{186}\text{W}$  and  $^{32}\text{S}+^{170}\text{Er}$  analyses will be presented in Secs. III C and III D. Details of the collective states of the target nuclei included in the coupled-channels calculations are given later in the text for each reaction. For the projectile, couplings to the first excited  $2^+$  state in  $^{32}\text{S}$  has a negligible effect in the determination of the diffuseness parameter. However, for some cases, a calculation which includes projectile and target excitations can lead to numerical instabilities. Thus, for all reactions studied here, the projectile  $^{32}\text{S}$  has been treated as inert in the coupled-channels analysis.

### A. The $^{32}\text{S}+^{208}\text{Pb}$ reaction

Figure 3 shows the experimental quasi-elastic excitation function for the  $^{32}\text{S}+^{208}\text{Pb}$  reaction. By performing a single-channel analysis, the best fit to the quasi-elastic data is achieved for a value for the surface diffuseness parameter  $a = 0.75 \pm 0.02$  fm, as represented by the solid line in Fig. 3. As we might expect from Fig. 2, this result is significantly larger than the diffuseness parameter value reported in Ref. [10] ( $a = 0.60 \pm 0.04$  fm). The solid lines in Figs. 4(b) and 4(b) indicate the best fits to the measurements with diffuseness parameters of  $a = 0.65$  and  $a = 0.85$  fm, respectively. It is evident that the calculated energy dependence obtained with these diffuseness values are inconsistent with the experimental data. Clearly, the high precision quasi-elastic scattering data presented in this work provide an outstanding test of the surface characteristics of the nuclear potential.

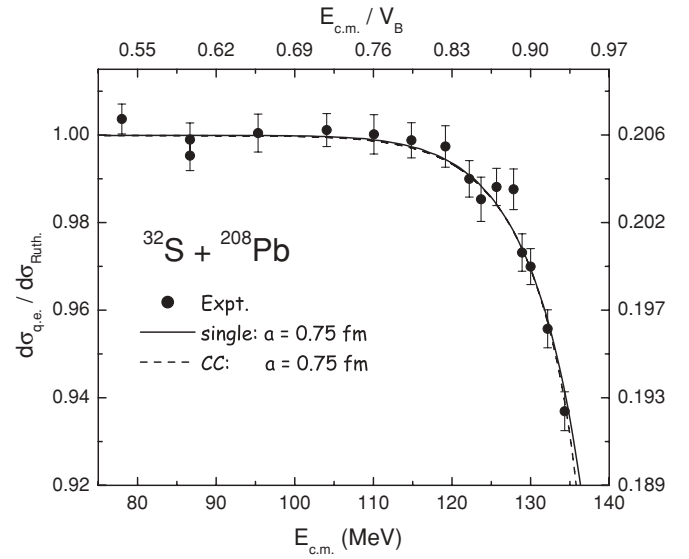


FIG. 3. Ratio of the quasi-elastic scattering to the Rutherford cross section measured at  $\theta = 174^\circ$  for the  $^{32}\text{S}+^{208}\text{Pb}$  reaction. The solid line represents the results obtained from a single-channel analysis, whereas the dashed line (almost coinciding with the solid line) corresponds to coupled-channels calculations. The diffuseness parameter was obtained by performing a least-squares fit to the data.

The experimental quasi-elastic scattering excitation function was also compared with coupled-channels calculations. Couplings to the  $3^-$ ,  $5^-$ , and double octupole-phonon [21,22] states in  $^{208}\text{Pb}$  were included. The coupling strengths were obtained from experimental data [23], except for the double octupole-phonon state, which was calculated in the harmonic limit. The lowest collective states of  $^{208}\text{Pb}$ , the  $3^-$  and  $5^-$  states, have excitation energies  $\epsilon_2 = 2.615$  and  $\epsilon_3 = 3.198$  MeV. The target radius parameter  $r_t$  was taken to be 1.06 fm as in previous analyses [24]. The diffuseness parameter giving the best fit to the experimental quasi-elastic scattering data is identical to the one obtained by considering a single-channel potential. The results are indicated by the dashed line in Fig. 3. As expected, at deep sub-barrier energies, couplings play a negligible role in quasi-elastic reactions involving near-spherical nuclei, and their contribution can be totally disregarded.

### B. The $^{32}\text{S}+^{197}\text{Au}$ reaction

Figure 5 presents the experimental quasi-elastic excitation function for the  $^{32}\text{S}+^{197}\text{Au}$  reaction. The solid line in panel (a) was calculated using a single-channel potential with  $a = 0.79 \pm 0.03$  fm, which corresponds to the best  $\chi^2$  fit to the data. We also carried out coupled-channels calculations for the  $^{32}\text{S}+^{197}\text{Au}$  reaction. For  $^{197}\text{Au}$  we included rotational couplings with a  $\beta_2$  deformation parameter of 0.15 (calculated for  $r_t = 1.06$  fm), which was determined from the averaged value of  $\beta_2$  for the neighboring  $^{196}\text{Pt}$  and  $^{198}\text{Hg}$  nuclei. The energy of the first excited state (384 keV) was similarly obtained from averaging the excitation energies of the  $2^+$  states of the  $^{196}\text{Pt}$  and  $^{198}\text{Hg}$  nuclei. The nucleus

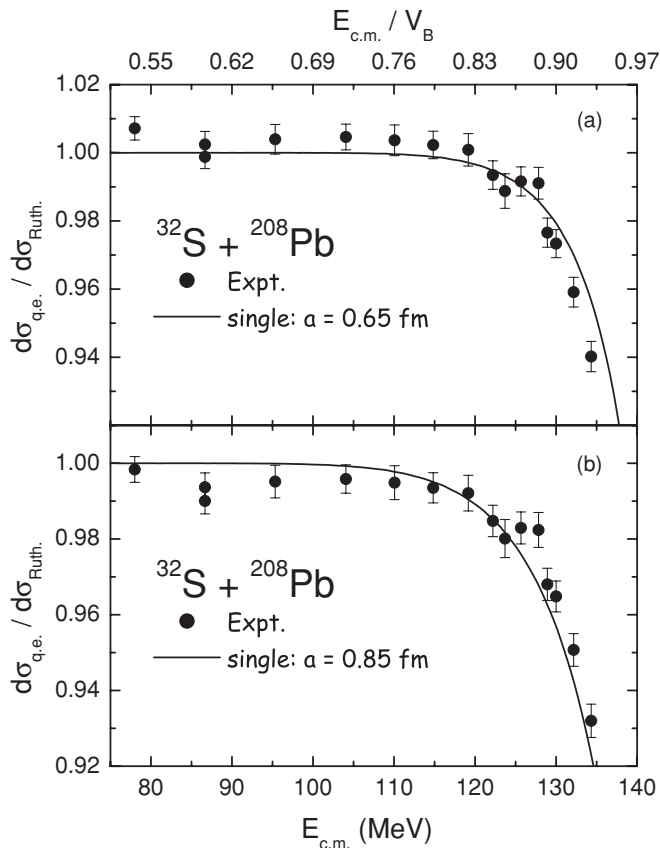


FIG. 4. Same as Fig. 3, but the solid line represents best fits obtained from a single-channel analysis with (a)  $a = 0.65$  fm and (b)  $a = 0.85$  fm.

$^{197}\text{Au}$  is not a good rotor and hence the coupling scheme is probably unrealistic. However, the main motivation in performing these coupled-channels calculations for  $^{32}\text{S}+^{197}\text{Au}$  is to ascertain whether different internal structure of the colliding nuclei has a significant effect on the quasi-elastic scattering cross section measured at energies well below the Coulomb barrier. In the fitting, couplings were considered to the first, second and third rotational states, after checking that including additional states in the couplings scheme does not change the calculated quasi-elastic scattering results. However, they can give rise to numerical instabilities, resulting in spurious values for the lowest energies. With couplings, the best value of the diffuseness parameter is  $a = 0.77 \pm 0.04$  fm, the calculation being indicated by the dashed line in Fig. 5(a). The diffuseness parameter was found to stay within its error bar limits if one increased the magnitude of the  $\beta_2$  deformation parameter for  $^{197}\text{Au}$  by 20%. The values of the diffuseness parameter obtained with the single-channel and coupled-channels analysis are in good agreement with each other, indicating that the overall effects of couplings on quasi-elastic scattering are minimal at such low energies.

In Ref. [10], Washiyama *et al.* reported that quasi-elastic analysis should be restricted to values of  $d\sigma_{q.e.}/d\sigma_{Ruth.}$  above 0.94, since below this value the quasi-elastic flux is depleted because of fusion, which depends sensitively on couplings. This criterion is somewhat arbitrary, but as will become

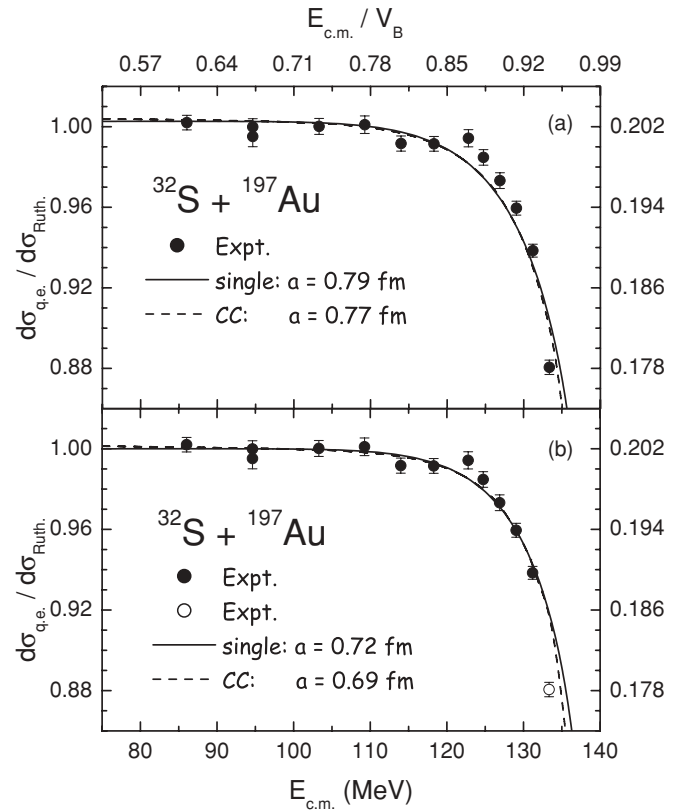
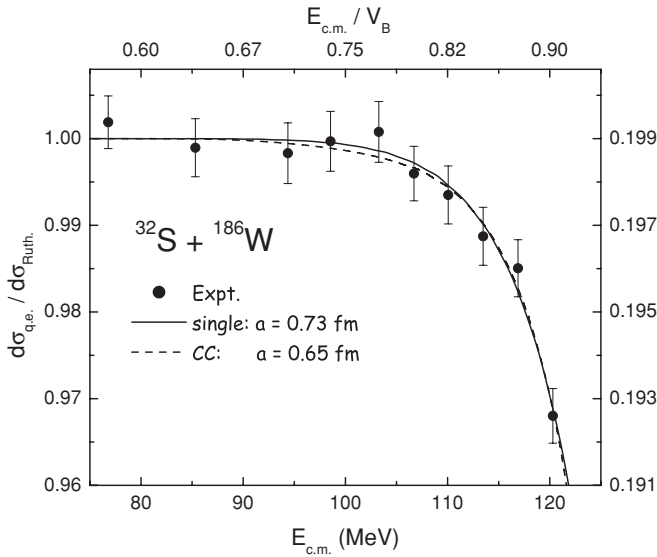


FIG. 5. (a) Same as Fig. 3, but for the  $^{32}\text{S}+^{197}\text{Au}$  reaction. (b) The solid line shows the fit obtained with a single-channel potential, without considering the highest energy data point (open circle).

clear the conclusions of our work are not affected by this particular choice. If the highest energy point is omitted from the experimental quasi-elastic excitation function in the  $\chi^2$ -fitting procedure, the best fitted diffuseness parameter obtained with a single-channel analysis becomes  $a = 0.72 \pm 0.02$  fm, which is in close agreement with the value obtained for  $^{32}\text{S}+^{208}\text{Pb}$ . Again, this result is larger than the diffuseness parameter value reported in Ref. [10] ( $a = 0.57 \pm 0.04$  fm). The corresponding results are as shown by the solid line in Fig. 5(b). The open circle in the figure indicates the quasi-elastic scattering measurement not included in the fit. Excluding this highest energy data point, the coupled-channels analysis leads to  $a = 0.69 \pm 0.02$  fm, as represented by the dashed line in Fig. 5(b). Including all data points in the analysis, both single-channel and coupled-channels fits result in values of  $\chi^2/n$  of around 5.9. The quality of the fit is significantly improved if the highest energy data point is omitted, although the diffuseness parameter which best fits the data only changes by about 9%.

### C. The $^{32}\text{S}+^{186}\text{W}$ reaction

The experimental quasi-elastic scattering results for the  $^{32}\text{S}+^{186}\text{W}$  system are shown in Fig. 6. The solid line in the figure indicates the result of the best-fitting single-channel nuclear potential with diffuseness parameter  $a = 0.73 \pm 0.03$  fm. This result is in good agreement with the diffu-

FIG. 6. Same as Fig. 3, but for the  $^{32}\text{S}+^{186}\text{W}$  reaction.

ness parameter values obtained for  $^{32}\text{S}+^{208}\text{Pb}$  ( $a = 0.75 \pm 0.02$  fm) and  $^{32}\text{S}+^{197}\text{Au}$  ( $a = 0.72 \pm 0.02$  fm), the latter obtained by omitting the highest energy quasi-elastic scattering data point.

In the coupled-channels analysis, rotational couplings for  $^{186}\text{W}$  were included, the target radius parameter was taken to be  $r_t = 1.06$  fm, and a total of five rotational states were considered, with  $\beta_2$  and  $\beta_4$  deformation parameters of 0.29 [25] and  $-0.03$  [26]. The experimental energy of the first excited  $2^+$  state is 123 keV. As shown by the dashed line in Fig. 6, the best-fitting diffuseness parameter is  $a = 0.65 \pm 0.03$  fm. To investigate the effect of varying the target radius parameter, we performed coupled-channels calculations with  $r_t = 1.2$  fm, with the quadrupole deformation parameter being changed accordingly ( $\beta_2 = 0.23$ ). As a result, the value for the best-fit diffuseness parameter increases by only 0.01 fm. Fits for both radius parameters were also carried out by setting the  $\beta_4$  value to zero, resulting in an almost unchanged value of the diffuseness parameter.

Although the diffuseness parameter obtained with the coupled-channels analysis is about 11% smaller than that obtained with a single-channel potential, both calculations give equally satisfactory fits to the quasi-elastic scattering data. The difference in the values of diffuseness parameters is possibly related to the fact that couplings change the shape of the quasi-elastic excitation function, as will become more apparent for the  $^{32}\text{S}+^{170}\text{Er}$  reaction, which has a large quadrupole deformation.

#### D. The $^{32}\text{S}+^{170}\text{Er}$ reaction

Among the reactions studied in this paper,  $^{32}\text{S}+^{170}\text{Er}$  is the most favorable for testing the influence of couplings on the quasi-elastic scattering yields. Figure 7 shows the measured quasi-elastic scattering excitation function for the  $^{32}\text{S}+^{170}\text{Er}$  reaction. In the coupled-channels analysis, a total of five rotational states were considered. The calculations made for

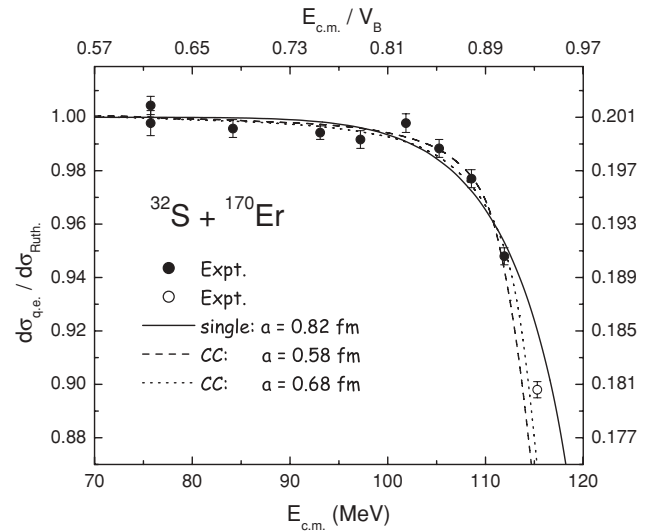


FIG. 7. Same as Fig. 3, but for the  $^{32}\text{S}+^{170}\text{Er}$  reaction. The solid line corresponds to the fit without couplings. The dashed and dotted lines are the ratio of the quasi-elastic scattering to the Rutherford cross section obtained using a coupled-channels analysis, with the target radius parameter taken to be 1.06 fm and 1.2 fm, respectively (see text for details). All theoretical fits were obtained without considering the highest energy data point (open circle).

$r_t = 1.06$  fm used  $\beta_2 = 0.43$  [25]. The best fit is indicated by the dashed line in Fig. 7, for which the diffuseness parameter is  $a = 0.58 \pm 0.02$  fm, obtained when the highest energy data point (open circle in Fig. 7) is omitted.

Taking  $r_t = 1.2$  fm, and correspondingly  $\beta_2 = 0.34$  [see Eq. (1)], the best fitted diffuseness parameter becomes  $a = 0.68 \pm 0.03$  fm, as shown in Fig. 7 by the dotted line. The use of a larger value of the target radius parameter in the coupled-channels analysis leads to a considerable increase in the diffuseness parameter. In particular, for the  $^{32}\text{S}+^{170}\text{Er}$  reaction, it may be more appropriate to give the lower and the upper limits of the diffuseness parameter obtained using coupled-channels calculations. At first glance, it might seem that the strong dependence of the diffuseness parameter on  $r_t$  and  $\beta_\lambda$  represents a drawback of the method. On the other hand, it is remarkable that quasi-elastic scattering excitation functions measured with very high precision are sensitive to somewhat small changes in the couplings strength of collective states in the coupled-channels analysis. As new precise quasi-elastic data are becoming available, the main uncertainties in the determination of the nuclear potential are mainly related to the limitations of model calculations (e.g., different values of  $r_t$  used in the coupled-channels analysis), and also to the uncertainty in the fusion barrier energy in some cases.

Performing a single-channel analysis, the best description of quasi-elastic scattering data is obtained with a significantly larger value of diffuseness  $a = 0.82 \pm 0.03$  fm (see solid line in Fig. 7). Fitting the data within a coupled-channels framework results in a better value of  $\chi^2$  than that obtained with a single-channel analysis (see Table II). If the highest energy data point is included in the analysis, the discrepancy

TABLE II. Diffuseness parameters (in fm) extracted from single-channel (SC) and coupled-channels (CC) analyses.  $n$  is the total number of quasi-elastic data points for each reaction.

Reaction <sup>a</sup>	$a$ (SC)	$\chi^2/(n-1)$	$a$ (CC)	$\chi^2/(n-1)$
$^{32}\text{S}+^{208}\text{Pb}$	$0.75 \pm 0.02$	0.75	$0.75 \pm 0.02$	0.72
$^{32}\text{S}+^{197}\text{Au}$	$0.72 \pm 0.02$	0.90	$0.69 \pm 0.02$	0.82
$^{32}\text{S}+^{186}\text{W}$	$0.73 \pm 0.03^b$	0.23	$0.65 \pm 0.03$	0.20
$^{32}\text{S}+^{170}\text{Er}$	$0.82 \pm 0.03^b$	1.82	$0.58 \pm 0.02^c$	0.78
			$0.68 \pm 0.03^d$	1.22

<sup>a</sup>Limiting to data points where  $d\sigma_{\text{q.e.}}/d\sigma_{\text{Ruth.}}$  is larger than 0.94, see text.

<sup>b</sup>Deformation effects are important, see text.

<sup>c</sup>Determined with  $r_t = 1.06$  fm and  $\beta_2 = 0.43$ .

<sup>d</sup>Determined with  $r_t = 1.20$  fm and  $\beta_2 = 0.34$ .

between the diffuseness parameter obtained with and without including couplings becomes even larger (the corresponding results are not shown in Fig. 7).

#### IV. DISCUSSION

The diffuseness parameters obtained in this work are summarized in Table II. The possible causes for the discrepancy between the results obtained with single-channel and coupled-channels analyses are discussed below.

##### A. Sensitivity of quasi-elastic scattering to Coulomb potential

The effect of couplings is most clearly seen by comparing the coupled-channels results with the best fit obtained from the single-channel calculations for the  $^{32}\text{S}+^{170}\text{Er}$  reaction. For energies larger than 100 MeV, the shapes of single-channel and coupled-channels calculations were found to be very different, the latter giving a better description of the data. To investigate whether the difference arises mainly from the use of a spherical Coulomb potential in the single-channel fits, the nuclear potential was turned off in both calculations. Figure 8 illustrates the calculated quasi-elastic scattering for the  $^{32}\text{S}+^{170}\text{Er}$  reaction. The solid circles represent the results obtained without couplings, for no nuclear potential. As expected, a single-channel analysis predicts values of quasi-elastic scattering which are very close to Rutherford for all incident energies when a spherical Coulomb potential is used. On the other hand, coupled-channels calculations incorporating the effects of deformation in the Coulomb potential deviate from unity by up to 1%, as indicated by the solid squares in Fig. 8. The deviations between the two calculations are apparent even at very low energies. These results clearly demonstrate that using a spherical Coulomb potential when fitting our high precision quasi-elastic data for reactions involving nuclei with large deformation is inadequate and will lead to incorrect interpretation. Including the nuclear potential, the results are only affected at the higher energies as would be expected. This is shown by the dotted line in Fig. 8, also shown in Fig. 7.

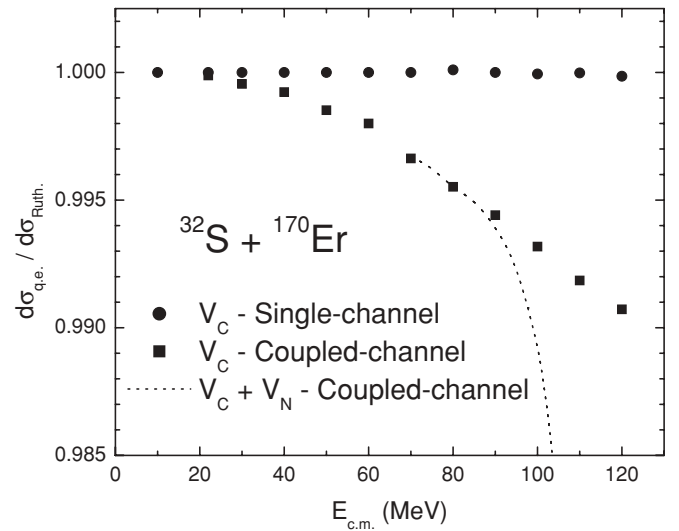


FIG. 8. Ratio of the calculated quasi-elastic scattering to the Rutherford cross section for the  $^{32}\text{S}+^{170}\text{Er}$  reaction. The solid circles represent the results obtained from a single-channel analysis; the solid squares correspond to coupled-channels calculations. Both results were obtained under the condition of vanishing of the nuclear potential. The dotted line presented here is also shown in Fig. 7.

In general, for the reactions between deformed nuclei, the diffuseness parameter required to describe the measured quasi-elastic scattering cross sections has to be larger in the absence of couplings. In part, this larger diffuseness counterbalances the suppression in  $d\sigma_{\text{q.e.}}/d\sigma_{\text{Ruth.}}$  caused by the deformed Coulomb potential. A simple way to verify the influence of deformation due to the Coulomb interaction in the single-channel analysis is by rescaling the calculated quasi-elastic scattering cross sections obtained with a single-channel potential by  $f(E) = (1.005 - 1.194) \times 10^{-4} E$ . The scale factor  $f(E)$  was obtained through a least-squares fit to the results presented in Fig. 8 by the solid squares between the energy range of 70–120 MeV. In this case, the best description of quasi-elastic scattering data for the  $^{32}\text{S}+^{170}\text{Er}$  reaction is obtained with  $a = 0.79 \pm 0.03$  fm, only 0.03 fm smaller than previously. This result is still far from the coupled-channels best fit value of  $0.68 \pm 0.03$  fm. From this we infer that the effect of including deformation in the nuclear interaction is also very important in the determination of the diffuseness parameter and is likely to further reduce the differences between single-channel and coupled-channels calculations. Accounting for the effects of deformation in the Coulomb potential alone is not sufficient, and a coupled-channels calculation seems necessary for reactions of nuclei with large static deformations.

##### B. Comparison between the diffuseness parameters obtained through single-channel and coupled-channels analysis

The diffuseness parameters extracted from single-channel and coupled-channels analyses (Table II) are plotted in Fig. 9 as a function of the charge product  $Z_1 Z_2$  of projectile and target. For the reactions involving near-spherical targets, the diffuseness parameters resulting from the single-channel and coupled-channels analyses are in good agreement. On the other

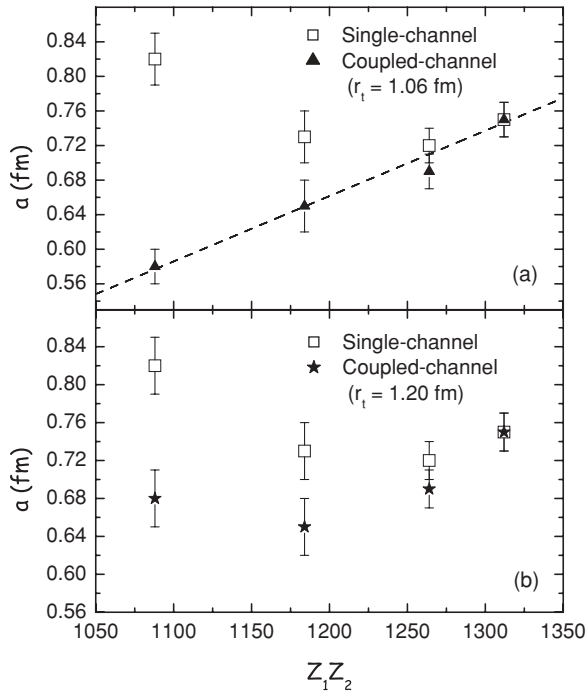


FIG. 9. Best fitted values of diffuseness parameter  $a$  as a function of the charge product of the projectile and target nuclei  $Z_1 Z_2$ . The open squares are the diffuseness values obtained with a single-channel potential. The diffuseness parameter values extracted from coupled-channels analysis with (a)  $r_t = 1.06$  fm (solid triangles) and (b)  $r_t = 1.20$  fm (solid stars) are also presented in the figure (see text for details).

hand, for the reactions with deformed targets, the discrepancy between the diffuseness parameters obtained from fits with and without couplings is significant. For the deformed reactions, the overall effect of couplings is to reduce the diffuseness parameter value required to fit the quasi-elastic scattering excitation function. As shown in Fig. 9, the larger the nucleus deformation, the larger the effect of couplings.

In Fig. 9(a), the diffuseness parameters are those obtained using coupled-channels fits with  $r_t = 1.06$  fm. The trend is illustrated by the dashed line, which is a least-squares fit. The diffuseness parameter appears to increase with the reaction charge product. However, the static deformation decreases with  $Z_1 Z_2$ . Taking  $r_t = 1.20$  fm in the coupled-channels analysis does not change the diffuseness parameter for the reactions with the near-spherical target nuclei. However, as shown in Fig. 9(b), it leads to an increase of 0.10 fm in the diffuseness parameter for the  $^{32}\text{S}+^{170}\text{Er}$  reaction, reducing the discrepancy between the results obtained with single-channel and coupled-channels analyses. This fact is perhaps not surprising, as the larger the target radius parameter  $r_t$  the smaller the deformation parameter  $\beta_\lambda$ . Note that for negligible values of deformation parameters, the single-channel and coupled-channels analyses are equivalent, which therefore results in equal values for the diffuseness parameter. The effect of using a larger value of  $r_t$  in the coupled-channels analysis is almost negligible for the  $^{32}\text{S}+^{186}\text{W}$  reaction, increasing the corresponding diffuseness parameter value by only 0.01 fm.

Considering all the reactions studied here, coupled-channels calculations using  $r_t = 1.20$  fm results in a weighted average diffuseness parameter of  $a = 0.70 \pm 0.01$  fm.

This work indicates that the nuclear potential outside the barrier radius is well represented by a WS form with  $a \simeq 0.60$ – $0.75$  fm. On the other hand, for the charge products  $Z_1 Z_2$  of the projectile and targets studied in this paper ( $1088 \leq Z_1 Z_2 \leq 1312$ ), the values of diffuseness required to describe above-barrier fusion cross sections range between approximately 1.15 and 1.25 fm. Those values of diffuseness were determined from the trend of all the data analyzed in Ref. [7], shown by the dashed line in Fig. 12(a) of Ref. [7]. From the present work, the origin of the anomalously large values for diffuseness parameter required to reproduce above-barrier fusion cannot be attributed to the unexpected behavior of the WS nuclear potential outside the barrier radius. Thus explanations in terms of deviations from the WS nuclear potential at closer distances and/or dissipative processes encountered during fusion may be necessary [7,8]. Further experimental and theoretical investigation is required.

## V. CONCLUSION

High precision deep sub-barrier quasi-elastic scattering excitation functions for the reactions of  $^{32}\text{S}$  with  $^{208}\text{Pb}$ ,  $^{197}\text{Au}$ ,  $^{186}\text{W}$ , and  $^{170}\text{Er}$  have been measured at backward angles. The investigation of the surface diffuseness parameter of the nuclear potential through the quasi-elastic scattering process requires data with high accuracy ( $\ll 1\%$ ) and careful measurements to minimize possible systematic uncertainties. The data were fitted to extract the diffuseness parameter with the constraint that experimental or interpolated fusion barrier energies for the different target nuclei have to be reproduced. Thus, for a given value of diffuseness, the potential parameters were varied so that the barrier energy was reproduced in each case. Since the absolute normalization of the experimental data is itself determined from calculated scattering, the normalization factor between the calculation and the data was allowed to vary freely in the  $\chi^2$ -fitting procedure. Single-channel fits to quasi-elastic scattering data give diffuseness parameters in the range of 0.72–0.82 fm, but these results should be taken with caution. A coupled-channels analysis results in the same values of the diffuseness for the near-spherical systems, but for reactions involving deformed targets, the inclusion of couplings in the calculations reduces the diffuseness parameter required to fit the experimental data. This work indicates that for reactions with deformed targets, the quasi-elastic data are sensitive to coupling effects even at energies well below the fusion barrier. In particular, the influence of couplings on quasi-elastic scattering is more apparent for the  $^{32}\text{S}+^{170}\text{Er}$  reaction, since  $^{170}\text{Er}$  has a large quadrupole deformation. Coupled-channels fits to quasi-elastic scattering cross sections result in diffuseness parameters in the range of 0.58–0.75 fm. These values of the diffuseness parameter are close to those expected from double-folding model calculations and elastic scattering systematics, but they are much smaller than those required to fit above-barrier fusion cross sections. For the



reactions studied in this work, the diffuseness parameters obtained from above-barrier fusion studies [7] range between 1.15 and 1.25 fm, which are almost twice those found here. The reason for this disagreement is still an open question, and further investigations are currently in progress. These high precision data, combined with the high precision fusion data already available, present a challenge to future realistic models which should explain simultaneously all reaction processes.

#### ACKNOWLEDGMENTS

The authors would like to thank Dr. K. Washiyama for helpful suggestions. L.R.G is grateful to L. C. Chamon for fruitful discussions. This work was supported by the Australian Research Council. P.R.S.G. and R.M.A. acknowledge the financial support from CNPq and PRONEX/FAPERJ. The work of K.H. was supported by the Grant-in-Aid for Scientific Research, Contract No. 19740115, from the Japanese Ministry of Education, Culture, Sports and Technology.

- 
- [1] R. A. Broglia and A. Winther, *Heavy Ion Reactions*, in Frontiers in Physics Lecture Note Series (Addison-Wesley, Redwood City, CA, 1991), Vol. 84.
- [2] P. R. Christensen and A. Winther, *Phys. Lett.* **B65**, 19 (1976).
- [3] M. Lozano and G. Madurga, *Nucl. Phys.* **A334**, 349 (1980).
- [4] L. C. Chamon, D. Pereira, E. S. Rossi, C. P. Silva, H. Dias, L. Losano, and C. A. P. Ceneviva, *Nucl. Phys.* **A597**, 253 (1996).
- [5] M. A. G. Alvarez, L. C. Chamon, D. Pereira, E. S. Rossi, C. P. Silva, L. R. Gasques, H. Dias, and M. O. Roos, *Nucl. Phys.* **A656**, 187 (1999).
- [6] C. P. Silva *et al.*, *Nucl. Phys.* **A679**, 287 (2001).
- [7] J. O. Newton, R. D. Butt, M. Dasgupta, D. J. Hinde, I. I. Gontchar, C. R. Morton, and K. Hagino, *Phys. Rev. C* **70**, 024605 (2004).
- [8] A. Mukherjee, D. J. Hinde, M. Dasgupta, K. Hagino, J. O. Newton, and R. D. Butt, *Phys. Rev. C* **75**, 044608 (2007).
- [9] K. Hagino, T. Takehi, A. B. Balantekin, and N. Takigawa, *Phys. Rev. C* **71**, 044612 (2005).
- [10] K. Washiyama, K. Hagino, and M. Dasgupta, *Phys. Rev. C* **73**, 034607 (2006).
- [11] O. A. Capurro, J. O. Fernández Niello, A. J. Pacheco, and P. R. S. Gomes, *Phys. Rev. C* **75**, 047601 (2007).
- [12] M. Dasgupta, D. J. Hinde, N. Rowley, and A. M. Stefanini, *Annu. Rev. Nucl. Part. Sci.* **48**, 401 (1998).
- [13] A. B. Balantekin and N. Takigawa, *Rev. Mod. Phys.* **70**, 77 (1998).
- [14] T. J. Schuck, H. Timmers, and M. Dasgupta, *Nucl. Phys.* **A712**, 14 (2002).
- [15] D. J. Hinde, M. Dasgupta, N. Herrald, R. G. Neilson, J. O. Newton, and M. A. Lane, *Phys. Rev. C* **75**, 054603 (2007).
- [16] C. R. Morton, A. C. Berriman, R. D. Butt, M. Dasgupta, D. J. Hinde, A. Godley, J. O. Newton, and K. Hagino, *Phys. Rev. C* **64**, 034604 (2001).
- [17] O. Akyüz and A. Winther, in *Nuclear Structure and Heavy-Ion Physics*, Proceedings of the International School of Physics, "Enrico Fermi", Course LXXVII, Varenna, 1979, edited by R. A. Broglia, C. H. Dasso, and R. Richi (North-Holland, Amsterdam, 1981).
- [18] K. Hagino (private communication).
- [19] J. O. Newton, C. R. Morton, M. Dasgupta, J. R. Leigh, J. C. Mein, D. J. Hinde, H. Timmers, and K. Hagino, *Phys. Rev. C* **64**, 064608 (2001).
- [20] K. Hagino, N. Rowley, and A. T. Kruppa, *Comput. Phys. Commun.* **123**, 143 (1999).
- [21] M. Yeh, P. E. Garrett, C. A. McGrath, S. W. Yates, and T. Belgya, *Phys. Rev. Lett.* **76**, 1208 (1996).
- [22] M. Dasgupta, K. Hagino, C. R. Morton, D. J. Hinde, J. R. Leigh, N. Takigawa, H. Timmers, and J. O. Newton, *J. Phys. G* **23**, 1491 (1997).
- [23] M. J. Martin, *Nucl. Data Sheets* **47**, 797 (1986).
- [24] M. Dasgupta, P. R. S. Gomes, D. J. Hinde, S. B. Moraes, R. M. Anjos, A. C. Berriman, R. D. Butt, N. Carlin, J. Lubian, C. R. Morton, J. O. Newton, and A. Szanto de Toledo, *Phys. Rev. C* **70**, 024606 (2004).
- [25] S. Raman, C. W. Nestor, Jr., and P. Tikkanen, *At. Data Nucl. Data Tables* **78**, 1 (2001).
- [26] J. R. Leigh, M. Dasgupta, D. J. Hinde, J. C. Mein, C. R. Morton, R. C. Lemmon, J. P. Lestone, J. O. Newton, H. Timmers, J. X. Wei, and N. Rowley, *Phys. Rev. C* **52**, 3151 (1995).